



University of HUDDERSFIELD

University of Huddersfield Repository

Abdul-Rahman, Hussein S., Lou, Shan, Zeng, Wenhan, Jiang, Xiang and Scott, Paul J.

Freeform texture representation and characterisation based on triangular mesh projection techniques

Original Citation

Abdul-Rahman, Hussein S., Lou, Shan, Zeng, Wenhan, Jiang, Xiang and Scott, Paul J. (2016) Freeform texture representation and characterisation based on triangular mesh projection techniques. *Measurement*, 92. pp. 172-182. ISSN 0263-2241

This version is available at <http://eprints.hud.ac.uk/id/eprint/28666/>

The University Repository is a digital collection of the research output of the University, available on Open Access. Copyright and Moral Rights for the items on this site are retained by the individual author and/or other copyright owners. Users may access full items free of charge; copies of full text items generally can be reproduced, displayed or performed and given to third parties in any format or medium for personal research or study, educational or not-for-profit purposes without prior permission or charge, provided:

- The authors, title and full bibliographic details is credited in any copy;
- A hyperlink and/or URL is included for the original metadata page; and
- The content is not changed in any way.

For more information, including our policy and submission procedure, please contact the Repository Team at: E.mailbox@hud.ac.uk.

<http://eprints.hud.ac.uk/>

Freeform texture representation and characterisation based on triangular mesh projection techniques

Hussein S Abdul-Rahman¹, Shan Lou¹, Wenhan Zeng¹, Xiangqian Jiang¹, Paul J. Scott¹

¹EPSRC Centre for Innovative Manufacturing in Advanced Metrology, Centre for Precision Technologies, School of Computing and Engineering, University of Huddersfield, Huddersfield

HD1 3DH

United Kingdom

Abstract

Texture characterisation for freeform non-Euclidean surfaces is becoming increasingly important due to the widespread of the use of such surfaces in different applications, e.g. the additive manufacturing. Four main steps are required to analyse and characterise those surfaces which include new surface representation, surface filtration and decomposition, texture representation methods and finally the calculation of the surface parameters. Recently, the representation, as well as the filtration and decomposition, of freeform surfaces have been investigated and some algorithms have been proposed. This paper, however, shed the light on how to represent the texture of freeform non-Euclidean surfaces before calculating the parameters. A novel model for freeform surface parameterisation is introduced; this new model proposes the use of a projection algorithm before the actual calculation of the parameters. Different projection algorithms have been adopted from the mesh projection techniques found in the field of computer graphics. The results of applying those algorithms to represent the texture of both simulated and bio-engineering surfaces are shown, also a comparison between those algorithms has been carried out. Furthermore, examples of calculating some of the surface parameters for freeform surfaces are given.

Keywords: freeform surfaces; non-Euclidean geometry, triangular meshes; surface characterisation; texture representation, surface metrology, geometrical metrology.

1. Introduction

Surface texture characterisation for traditional Euclidean planar surfaces is well established. The Euclidean surfaces are defined by a single height value for each point in a plane. Mature measurement instruments based on wide range of principles including interferometry, stylus, confocal microscopy, atomic-force microscopy and many other principles, have been applied to measure a variety of surfaces in many different applications. However, freeform non-Euclidean surfaces are rapidly emerging and they have been used in a number of different applications. For example, freeform surfaces are employed in optics in the extremely large European telescope E-ELT, 3D printed surfaces, energy-efficient jet engines, aircraft turbine wings and reliable long life human joints implants. Therefore, it is becoming very important to develop reliable and accurate measurement routines/approaches that can better characterise freeform surfaces which have non-Euclidean natures. Consequently, surface texture characterisation has witnessed important shifts in the last decade or two; from profile measurements to areal measurements and from simple surfaces to complex freeform surfaces [1-3]. These shifts have triggered the need for new algorithms and techniques that can better describe, represent, measure and characterise the newly evolved complex freeform surfaces [4-10].

Traditionally, the characterisation and parameterisation of surface texture is carried out using the four major steps namely: surface sampling and representation, decomposition and filtration, texture representation and mapping and finally surface parameterisation as shown in Figure 1. However, moving from simple geometries to complex freeform geometries requires the re-thinking and re-designing of the algorithms used in every step shown in the figure as many of the techniques that are used already are only valid for Euclidean surfaces.

Freeform surfaces have a more complex nature. The underlying domain is no longer a plane and contains points that have non-zero curvature, therefore, is called non-Euclidean; such freeform surfaces are also called non-Euclidean surfaces. According to Gauss's theorem in differential geometry, Theorema Egregium, surfaces with the same curvature can be mapped into each other without any distortion. In contrast, Surfaces with different curvature cannot be mapped into each other without distortion, for example, the Earth cannot be displayed on a planner map without distortion. Subsequently, a freeform non-Euclidean surface cannot be projected onto a plane without distortion or loss of some surface information. As a result, freeform surfaces can no longer be represented as a height values over a two-dimensional grid. To give another example, if attempts are made to represent a hemisphere surface over 2D grid, this will cause a distortion of the geodesic distances on the surface, i.e. the geodesic distances between different points on the actual surface will be distorted and will be smaller when projected onto the 2D grid. The geodesic distance between two points on a given surface is the shortest distance between the two points on that surface. Another example showing the invalidity of representing freeform non-Euclidean surfaces using 2D grid is that the lack of such method to represent closed surfaces such as a sphere.

Our research group has been working on redesigning each of the steps shown in figure 1 so that they will be valid to handle the non-Euclidean geometries found in the freeform surfaces. Therefore, a new representation

model based on three-dimensional triangular mesh was proposed to represent the freeform surfaces. This new representation method will preserve more information of the surface than the traditional method, height values over a regular grid, and will give extra flexibility to represent more surfaces that could not be represented before. Moreover, many filtering and decomposition algorithms for freeform surfaces that are represented by triangular meshes were proposed. Those algorithms use different principles such as partial differential equations, lifting wavelets, mesh relaxation schemes, morphological operations and manifold harmonics, to filter any freeform surface or decompose it into its different scales and components [4-10]. The work carried out in this paper continues the previous work by investigating the two remaining blocks in figure 1, i.e., the texture representation and the parameter calculation.

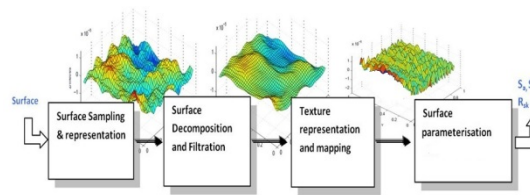


Figure 1 Surface characterisation model

One of the important aspects that need addressing for freeform surface characterisation is how to represent the texture of such surfaces, or in other words, how to represent the surface residues after filtering out the form. In simple geometries the assumption is that the form is Euclidean, i.e. a planar surface, therefore it will be easy to project the surface texture onto a plane and then analysing these residues to obtain surface parameters. This projection will not introduce any distortion because the form itself is assumed to be Euclidean. However, applying the same technique to freeform surfaces that have non-Euclidean geometries will introduce different types of distortions, either in the distances, angles or the areas of the original surface. Therefore, texture representation methods are very important in terms of minimising these types of distortions before analysing the surface and obtain its parameters.

In this paper, all non-Euclidean freeform surfaces are represented using 3D triangular mesh, therefore, using computer graphic terminology, the problem of projecting 3D triangular mesh into a 2D plane is also known as parameterisation, not to be confused with surface parameterisation in metrology with means calculating the surface parameters. Projection is a well-known problem within computer graphics society and many algorithms already exist attempting to solve this problem. A number of mesh projection techniques are investigated and applied to represent the texture of freeform non-Euclidean surfaces in this paper. However, prior to the application of these different projection techniques, it is of necessity to specify different types of metric distortion that may occur when projecting a freeform surface into a plane.

Metric distortion and surface projection techniques will be discussed in Section 2 of this paper. After the projection of the texture in a suitable planar two-dimensional domain, it is very important to calculate surface parameters that can describe the surface; the calculation of surface height parameters for the case of 3D

triangular meshes is discussed in Section 3. Computer generated and bioengineering case studies are shown in Section 4 of the paper.

2. Texture representation techniques for freeform surfaces

In this section, we will investigate a number of different 3D mesh projection methods that we will use to represent the texture of freeform surfaces. Mesh projection can be seen as the process of obtaining a map between a 3D triangular mesh in a three-dimensional domain and a 2D triangular mesh in a planar 2D domain. Projection algorithms are very popular research area in the field of computer graphics and many algorithms have been proposed. Examples of well-known projection algorithms can be found in the references [11-19].

Projection almost always introduces distortion in one or more surface metrics, i.e., surface angles, lengths and/or areas, and a good projection algorithm is the one which minimises one or more of these distortions. Therefore, the main goal of any projection algorithm is to minimise at least one of these distortions as we will see in throughout this section.

To better understand the distortion problem, a simple example that shows why projection algorithms are needed to represent the texture of freeform surfaces will be given in the following section. Then a number of basic and advanced projection algorithms will be discussed.

A. *Problems with traditional texture representation: an example*

After the decomposition of the surface and form removal process [4-10], the remaining residues that represent the surface texture have to be parameterised. The representation of these residues is very important for the calculation of the surface parameters. Traditionally, the texture is represented by subtracting the surface form from the actual surface. In the Euclidean surfaces, the surface form is a plane or very close to being planar. Therefore, residues can be accurately displayed with respect to a plane without having any distortion. To illustrate this, figure 2 gives an example of how the surface feature are not distorted with the traditional representation of the residues of a simple Euclidean surface. In the figure, the form is represented by the curved line, and the dots represent the surface textures or features and the straight solid line represents the projection plane. As shown in the figure, the distances between features or residues on the surface are the same distance between these residues in the projecting plane. Moreover, the error or the normal distance between the residues and the surface form are preserved in the projection plane. This means that one can calculate different texture parameters accurately based on this texture representation.

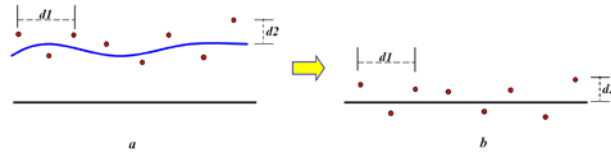


Figure 2 Texture representation for Euclidean surface; (a) the texture on the original surface and (b) the texture on a planar domain.

However, the traditional projection will be problematic when it comes to the non-Euclidean surfaces as distortion may occur. Figure 3 shows an example of the distortion that could arise if we project the non-Euclidean surface residues onto a planar domain using the traditional method. It is clear from the figure that the surface features are no longer preserved in this type of projection, for example, the distance between two residues on the surface is not the same as the distance between the same two residues on the projection plane, this can be seen in distance **d3** between two successive features on the surface which is significantly distorted and becomes smaller, distance **dd3** on the projection plane. Moreover, the normal distance between the surface form and the residue may also be distorted as could be seen in the difference in the distances **d4** and **dd4** on the surface and the projection plane respectively.

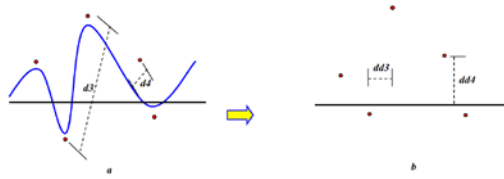


Figure 3 Texture representation for non-Euclidean surface; (a) texture on the original surface and (b) the texture on a planar domain.

From the previous example, it is evident that freeform surfaces will need projection algorithms that attempt to minimise surface metric distortions introduced due to the projection process.

B. Surface Metric distortion

It is very well established that surfaces can be represented using many different projection methods, and the projection of a given surface is not unique, and different projection will have different properties. For example, a hemisphere could be parameterised using different methods such as orthographic or stereographic projection [11, 19]. However, there are some intrinsic properties of the surface that are independent of the representation method, these intrinsic properties include the surface normals, Gaussian curvature and the mean curvature [11, 19]. Other properties, on the other hand, depend on the representation method, such as the angles, distances and areas on the surface. For example, only the stereographic projection of the hemisphere can preserve the angles of the hemisphere whereas the orthographic projection will cause the angles to be distorted [11].

The basic idea behind surface metric distortion is that, generally speaking, every small unit disc in the parameters 2D domain will be mapped into an ellipse in the actual 3D surface domain, as shown in figure 4 below. This transformation of circles into ellipses is called the local metric distortion of the projection method and the nature of this distortion is encoded into the length of the two major axes of the ellipse σ_1 and σ_2 shown in the figure.

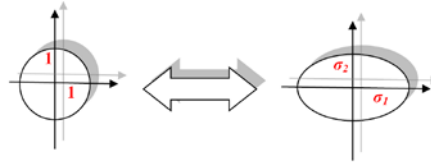


Figure 4 Surface metric distortions due to the transformation of circles into ellipses in the projection algorithm.

The values of σ_1 and σ_2 are in fact the two eigenvalues of the first fundamental form matrix, which derived from the Jacobian of the projection as defined in the field of differential geometry, more details about the first fundamental form matrix are given in [11, 19].

Based on the values of σ_1 and σ_2 , we can now summarise the main properties that a projection algorithm can have [11-13,19]:

- Isometric projection (distance-preserving), when $(\sigma_1 = \sigma_2 = \mathbf{1})$.
- Conformal projection (angle-preserving), when $(\sigma_1 = \sigma_2)$.
- Equiareal (area-preserving), when $(\sigma_1 \cdot \sigma_2 = \mathbf{1})$

In fact, the isometric mapping is conformal and equiareal, and this type of projection exists only for developed surfaces like planes, cones, and cylinders which have zero Gaussian curvature at all points of the surface. Therefore, it is very important to investigate different methods that would minimise metric distortions for freeform surfaces.

C. Fixed boundary representation algorithms

Fixed-boundary mapping, also known as Barycentric mapping [11-13, 19], is the simplest and fastest type of projection. In these algorithms, the 3D mesh surface is modelled by a network of springs that are connected at the vertices as shown in figure 5.

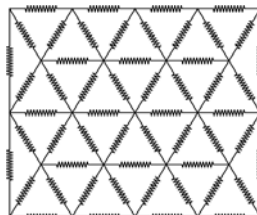


Figure 5 Spring network model for fixed boundary representation algorithms.

Therefore, projecting a surface into a plane can be carried out by stretching these springs in such a way that all vertices are located onto a plane with the most efficient configuration that would minimise the overall energy within all springs, which is given by [11]:

$$E = \frac{1}{2} \sum_{i=1}^n \sum_{j \in \mathcal{N}_i} D_{ij} \|\mathbf{u}_i - \mathbf{u}_j\|^2 \quad 1$$

Where D_{ij} represent the spring constant (weights) and is derived from the 3D mesh. \mathbf{u}_i is the parameterised location of the vertex i and \mathcal{N}_i is the first ring of neighbours of the vertex i in the original mesh.

The optimal solution that would minimise the total energy of the spring model is obtained when the vertices in the parametric domain are a weighted average of their neighbours [11-13, 19] as shown in figure 6 this relation can be expressed mathematically as:

$$\sum_{j \in \mathcal{N}_i} D_{ij} \mathbf{u}_j = \sum_{j \in \mathcal{N}_i} D_{ij} \mathbf{u}_i \quad 2$$

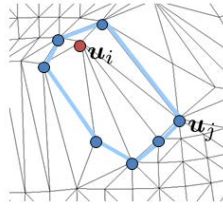


Figure 6 Fixed boundary vertices are a weighted average of their neighbours.

The question remains now is how to choose the spring constants, weights, D_{ij} in the spring model. The simplest choice of weights is $D_{ij} = 1$, another choice is that the weights to be proportional to the lengths of the corresponding edges in the triangular mesh. The main drawback of these two choices is that they do not minimise any of the metrics described earlier in the previous section. Other choices of weights that minimise the angular or distance distortion are:

- Discrete harmonic mapping [11]: in this type of mapping, the weights are derived from the approximation of the Laplacian operation (Laplace-Beltrami), these weights are given by:

$$D_{ij} = \frac{\cot \alpha_{i,j} + \cot \beta_{i,j}}{\sum_{l \in \text{even_ring}} \cot \alpha_{i,l} + \cot \beta_{i,l}} \quad 3$$

The discrete harmonic map will minimise the angular distortion, and it usually produces a good projection with relatively small angular distortion, except at the boundary, this method may give unexpected results and the bijectivity is not guaranteed. Bijectivity means that the projection is reversible and no flipping occurs in any of the triangles in the 2D mesh.

- Mean-value mapping [11-13]: this is another type of minimising angular distortion but using a different set of weights. In this case, the weights are given by:

$$D_{ij} = \frac{\tan(\frac{\alpha_{ij}}{2}) + \tan(\beta_{ij}/2)}{r_{i,j}} \quad 4$$

where, the angles α and β are the two opposite angles of the edge that connect the two vertices i and j , and $r_{i,j}$ is the length of that edge.

- Low-stretch mapping [14]: in this method, the weights are computed in two stages. In the first stage, the weights are calculated using the harmonic mapping or the mean-value as described above. For the second stage, the weights are updated using the eigenvalues of the first fundamental matrix σ , as explained in the previous section. The updated weights are given by:

$$D_{ij}(new) = \frac{D_{ij}(old)}{\sigma_j} \quad 5$$

Fixed-boundary mapping gives a fast and reliable projection that would minimise some of the metric distortions. However, this type of projection requires the boundary to be fixed on a convex hull which will cause big distortions at the boundaries. Various type of barycentric mapping is implemented and the results are shown in the following sections.

D. Free boundary representation algorithms

Projecting the texture of a freeform surface into a plane will always result in a distortion with one or more properties of the surface. Distortion free projection is only possible with developed surfaces that have zero curvature, i.e. Euclidean, and all other types of surfaces will suffer some type of distortion when projected onto a planar domain.

All fixed boundary algorithms discussed in the previous section require the boundary vertices to be fixed on a convex shape, such as a rectangle, circle, and triangle, which will lead to huge distortions near those boundaries.

In this section, however, a number of more advanced algorithms that do not require the boundaries to be fixed are investigated; such algorithms are sometimes called free boundary projection algorithms, and will produce a projection that has a minimum distortion in one or more metrics. Fortunately, the field of computer graphics is very rich with such algorithms. In this section, four well-known algorithms have been investigated and applied to represent the texture of free-form surfaces, these algorithms are; the least square conformal mapping (LSCM), the angle based flattening (ABF), the as-similar-as-possible algorithm (ASAP) and the as-rigid-as-possible algorithms (ARAP) [15-18].

All of the aforementioned algorithms attempt to minimise a cost function that measures an overall distortion function of the projection. The overall cost function is defined as the averaging of local distortions over the whole parametric domain Ω , where the local distortion is calculated over each triangle using the eigenvalues (σ_1, σ_2) . The overall cost function is mathematically expressed as:

$$E = \frac{\sum_{t \in \Omega} E(\sigma_1, \sigma_2)}{\sum_{t \in \Omega} A(t)} \quad 6$$

Where;

$E(\sigma_1, \sigma_2)$ is the local distortion at a particular triangle, which depends on the eigenvalues (σ_1, σ_2)

$A(t)$ is the area of that particular triangle.

Ω refers to the whole 2D parametric domain.

Least square conformal mapping defines the local distortion as the square different between the two eigenvalues [15] as:

$$E(\sigma_1, \sigma_2) = \frac{1}{2}(\sigma_1 - \sigma_2)^2 \quad 7$$

This local distortion is used in the global cost function shown in equation 8.6, and then the minimum solution is found using one numerical minimisation methods such as gradient descent. It is obvious that the minimum solution will occur when $(\sigma_1 = \sigma_2)$ which result in an angle-preserving projection. However, it has been found that the LSCM also produce a very local areal distortion. Nevertheless, the LSCM do not guarantee local or global bijectivity, and can theoretically result in flipped triangles and overlaps.

The as-similar-as-possible (ASAP) [16] algorithm tries to force each triangle in the parametric domain to be as similar as possible to its 3D counterpart. This algorithm uses the same local distortion as the conformal mapping and yields very close results to those of the LSCM algorithm.

The as-rigid-as-possible (ARAP) algorithm [16] tries to force each 2D triangle in the parametric domain to be as rigid as possible to its 3D counterpart. This projection attempt to minimise the stretch distortion by defining the local distortion as:

$$E(\sigma_1, \sigma_2) = (\sigma_1 - 1)^2 + (\sigma_2 - 1)^2 \quad 8$$

It is obvious that the minimum solution will occur only when $\sigma_1 = \sigma_2 = 1$. In other words, this projection attempts to preserve all the metrics of the original surface.

The angle based flattening (ABF) method, developed by Sheffer *et al* [17, 18], uses a different approach to obtain an angle-preserving projection. Instead of defining the overall cost function as an average of all local distortion; the cost function is defined here to be the difference between the angles in the 2D and 3D domains. The cost function for the ABF is given by:

$$E_{ABF}(\alpha) = \sum_{t \in \Omega} \sum_{k=1}^3 (\alpha_i^k - \phi_i^k)^2 \cdot \omega_i^k$$

9

Where;

α_i^k is an angle in the 2D parameter domain.

ϕ_i^k is an optimal angle, derived from the angles in the 3D mesh.

ω_i^k is weighting factor.

To ensure that the 2D angles define a valid triangulation, a set of constraints needs to be satisfied. The most two important constraints are designed to ensure that the sum of angles in a single triangle is π and the sum of the angles around an internal vertex should be equal to 2π .

Examples of different projection results for computer-generated as well as real engineering surfaces represented by 3D triangular meshes are shown and discussed later in this paper.

3. Calculations of global statistical characteristics of freeform surfaces

After representing the texture on the parametric domains, the texture parameters have to be calculated. Traditionally, the texture parameters are calculated on the basis that the surface is regularly sampled over a grid, this assumption is no longer valid for the case of freeform surfaces represented by 3D triangular meshes. In the case of the freeform surfaces, the calculations of surface parameters have to be generalised. In this section, four surface parameters that are widely used among different disciplines, *Sa*, *Sq*, *Ssk* and *Sku*, are extended for the case in triangular meshes. The definition of surface height parameters and many other parameters for traditional surfaces can be found in many books and research papers, for example [1-3, 20-21].

- The arithmetic mean height, *Sa*:

The arithmetic mean height or *Sa* parameter is defined as the arithmetic mean of the absolute value of the height in the normal direction over the parametric domain, the *Sa* for traditional surfaces is given by:

$$Sa = \frac{1}{A} \iint |z(x, y)| \cdot dx dy$$

10

The formula above can be understood as calculating the total sum of all volumes between the surface and the residues, and then dividing that total volume by the total area of the surface. Therefore, this formula can be extended to suit the case of triangular mesh, and for triangular mesh the *Sa* is given by:

$$S_a = \frac{\sum_{t \in \Omega} \left(A(t) \cdot \sum_{k=1}^3 \left(\frac{|z_{t,k}|}{3} \right) \right)}{\sum_{t \in \Omega} A(t)} \quad 11$$

Where;

$A(t)$ is the area of the triangle t in the parametric domain Ω as could be seen in figure 7.

$z_{t,k}$ is the residue value of the vertex k in the triangle t in the parametric domain Ω as could be seen in figure 7.

$\sum_{k=1}^3 \left(\frac{|z_{t,k}|}{3} \right)$, is the mean value of the surface residues (texture) for the three vertices of the triangle t

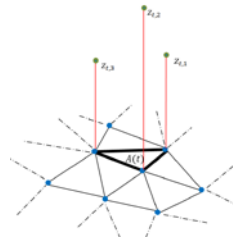


Figure 7 Calculating parameters for a surface represented by a 3D triangular mesh.

- The root mean square height, Sq :

The root mean square height or Sq parameter is defined as the root mean square value of the surface heights in the normal direction within the whole parametric domain, and it is given by:

$$Sq = \sqrt{\frac{\sum_{t \in \Omega} \left(A(t) \cdot \sum_{k=1}^3 \left(\frac{z_{t,k}^2}{3} \right) \right)}{\sum_{t \in \Omega} A(t)}} \quad 12$$

- The Skewness, Ssk :

Skewness is the ratio of the mean of the heights values of texture cubed, in the normal direction, to the cube of Sq within the parametric domain, or:

$$Ssk = \frac{\sum_{t \in \Omega} \left(A(t) \cdot \sum_{k=1}^3 \left(\frac{z_{t,k}^3}{3} \right) \right)}{Sq^3 \cdot \sum_{t \in \Omega} A(t)} \quad 13$$

- The Kurtosis, Sku :

The Sku parameter is a measure of the sharpness of the surface texture heights distribution in the normal direction and is the ratio of the mean of the fourth power of the normal texture height values of the fourth power of Sq within the parametric domain, and it can be expressed mathematically as:

$$Sku = \frac{\sum_{t \in \Omega} \left(A(t) \cdot \sum_{k=1}^3 \left(\frac{z_{t,k}^4}{3} \right) \right)}{Sq^4 \cdot \sum_{t \in \Omega} A(t)} \quad 14$$

4. Case studies

The aforementioned mesh projection algorithms have been investigated to represent the texture for a computer generated surfaces represented by triangular mesh and also to represent the texture of real measured surfaces. The results are shown and compared in the following subsections.

A. Computer generated surfaces

In order to compare between the different algorithms, three freeform computer generated surfaces represented by triangular mesh is created. These surfaces are designed to cover a wide range of freeform non-Euclidean surfaces with different topological types. The first surface is a saddle shaped surface which is considered to be a typical example of a non-Euclidean surface with a negative curvature. The second surface is a wavy surface that has more topological features than the first one. The third surface is a more complicated surface with non-constant curvatures to simulate a complex freeform surface; we refer to this surface as an egg-box surface. All of these surfaces are represented by triangular meshes and they are shown in figure 8.

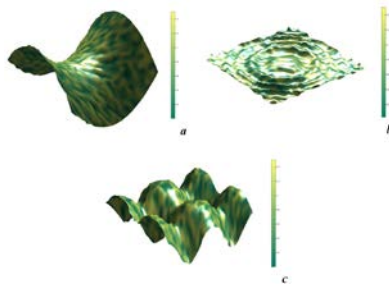


Figure 8 Computer-generated surfaces represented by 3D triangular meshes; (a) the saddle surface, (b) the wavy surface and (c) the egg-box surface.

Using the aforementioned mesh projection methods discussed in the previous section, these three surfaces are projected from 3-dimensional xyz domain into 2-dimensional UV domain and the results of these UV domains are shown in figures 9, 10 and 11.

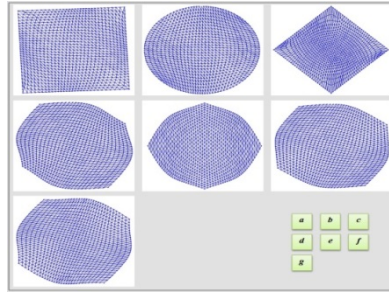


Figure 9 Projection results (UV-domains) of the saddle surface using: (a) square boundary harmonic projection, (b) circle boundary harmonic projection, (c) low-stretch projection, (d) LSCM projection, (e) ABF projection, (f) ASAP projection and (g) ARAP projection.

Figure 9 shows the UV domains of the saddle surface yield from different mesh projection algorithms. These algorithms have different results because each of these algorithms is attempting to minimise one particular metric error in the original surface. Figure 9(a) shows the UV domain of projecting the saddle surface onto a plane using the fixed boundary harmonic mapping with a square boundary, whereas figure 9(b) shows the UV domain of the fixed boundary harmonic mapping with a circular boundary. Fixed boundary harmonic mapping is designed to minimise the angular distortion of the original surface, and it generally gives good results in the middle regions of the surface but introduces big distortions at the boundary.

Figure 9(c) shows the UV domain of the saddle surface when using the fixed boundary low-stretch algorithm. This algorithm is designed to minimise the errors introduced in the distances of the original mesh. However, it might produce a higher angular distortion than the other algorithms as a cost of minimising the stretch error. Moreover, because this is a fixed boundary algorithm huge distortions will always be at the boundaries.

To minimise the error around the boundary, the advanced free boundary algorithms, namely, LSCM, ABF, ASAP and ARAP, described earlier are applied. Figures 9(d)-(g) show the UV domains of these algorithms respectively. As can be seen from the figure, these algorithms relaxed the boundary to minimise the distortion. Despite the fact that the LSCM, ABF and ASAP algorithms all attempts to minimise the angular distortion of the original mesh, they are using different strategies. Each of these algorithms defines an objective function that needed to be minimised slightly different that the other with may affect the overall minimization results.

As discussed earlier, mesh projection algorithms attempt to minimise the distortion of one of the intrinsic features of the original surface when projected onto a 2D plane. Table 1 below shows the root mean square errors of the angles, areas and length when projected onto a 2D parametric domain using different algorithms. The root mean square error is calculated by matching all the vertices and edges in the 3D surface domain to the corresponding vertices and edges in the 2D projection domain, and then calculating the areas, angles, and lengths to find the RMS differences between the two domains.

Table 1. Angles, areas, lengths root mean square errors between the 3D mesh and the 2D UV-planar mesh for the Saddle Surface

Projection Method	Angles RMS error (degree)	Areas RMS error (unit length ²)	Lengths RMS error (unit length)
Harmonic / square	0.1954	0.0332	0.2734
Harmonic / circle	0.0789	0.0319	0.2423
Low-Stretch	0.2876	0.0324	0.2388
LSCM	0.0509	0.0325	0.2521
ABF	0.0519	0.0345	0.2715
ASAP	0.0511	0.0323	0.2498
ARAP	0.0662	0.0322	0.2484

As can be seen from the table, angular based algorithms, e.g. the harmonic/circle, produce less error in the angular distortion but might produce higher errors in the other metrics and so for the areal and stretch algorithms as anticipated.

After calculating a 2D planar domain for a 3D surface, the surface texture that is extracted from analysing, filtering and decomposing the 3D surface [4-10], has to be projected back into this 2D planar domain so that the surface parameters can be calculated. Traditionally, the surface texture is projected onto a 2D planar domain by subtracting the surface form from the original surface. As mentioned earlier in the beginning of this paper, this type of simple projection which performed by only subtracting the form will result in distortion of surface metrics; angles, lengths or/and areas. Figure 10 shows the projection of the surface texture onto various UV-domains for the saddle surface.

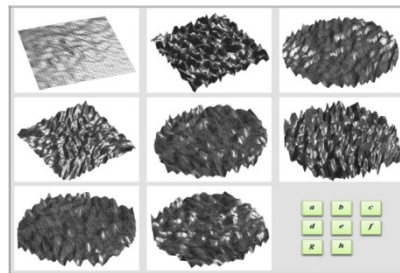


Figure 10 Surface texture imposed onto different UV-domains of the saddle surface using; (a) Traditional projection, (b) square boundary harmonic projection, (c) circle boundary harmonic projection, (d) low-stretch projection, (e) LSCM projection, (f) ABF projection, (j) ASAP projection and (h) ARAP projection.

Finally, different surface parameters could be calculated once the texture is projected into a suitable 2D planar domain. Table 2 shows a number of different surface parameters for the saddle surface calculated using the equations 11-14 as explained in the previous section.

Table 2. Some of the global statistical parameters for the for the Saddle Surface

Projection Method	Sa	Sq	Ssk	Sk_u
Traditional projection	0.0361	0.0488	1.7165	3.3650
Harmonic / square	0.0746	0.0865	1.3066	1.8227
Harmonic / circle	0.0746	0.0864	1.3063	1.8222
Low-Stretch	0.0741	0.0855	1.3025	1.8198
LSCM	0.0746	0.0865	1.3062	1.8223
ABF	0.0746	0.0865	1.3063	1.8224
ASAP	0.0747	0.0865	1.3059	1.8212
ARAP	0.0746	0.0864	1.3054	1.8198

As could be read from the table, all the parameters are close to each other. However, the traditional projection shows relatively different results than the other methods. As an example, the Sa and Sq parameters calculated using the traditional projection gives an indication that the surface is relatively smooth. Nevertheless, the parameters calculated using other projection methods show that the surface is actually rougher with higher Sa and Sq parameters. This example illustrates that the traditional projection method is on longer valid to calculate the parameters of the freeform surfaces.

The Projection results for the wavy and the egg-boxed surfaces can be seen in figures 11 to 14 below.

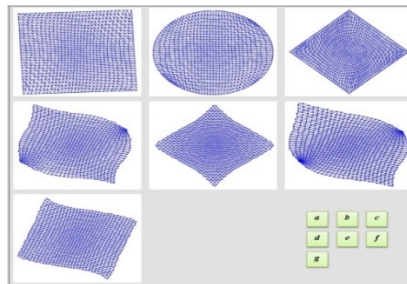


Figure 11 Projection results (UV-domains) of the wavy surface using; (a) square boundary harmonic projection, (b) circle boundary harmonic projection, (c) low-stretch projection, (d) LSCM projection, (e) ABF projection, (f) ASAP projection and (g) ARAP projection.

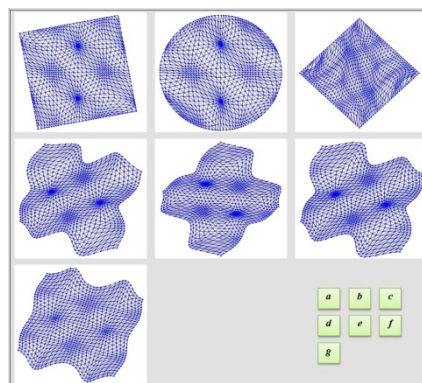


Figure 12 Projection results (UV-domains) of the egg-box surface using; (a) square boundary harmonic projection, (b) circle boundary harmonic projection, (c) low-stretch projection, (d) LSCM projection, (e) ABF projection, (f) ASAP projection and (g) ARAP projection.

Figures 13 and 14 show the results of projecting the texture of wavy and egg-box surfaces into various UV-domains. The root mean square RMS errors for the main surface metric between the 3D surface and its 2D counterpart are calculated in tables 3 and 4.

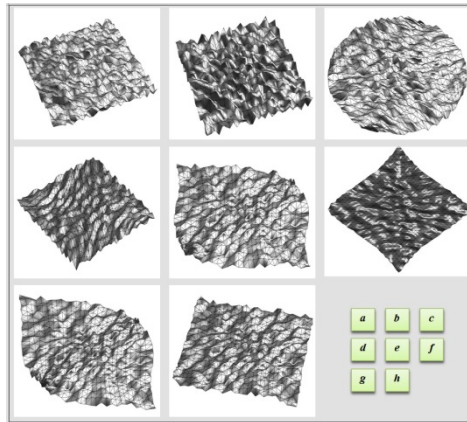


Figure 13 Surface texture imposed onto different UV-domains of the wavy surface using; (a) Traditional projection, (b) square boundary harmonic projection, (c) circle boundary harmonic projection, (d) low-stretch projection, (e) LSCM projection, (f) ABF projection, (j) ASAP projection and (h) ARAP projection.

Table 3. Angles, areas, lengths root mean square errors between the 3D mesh and the UV mesh for the wavy Surface

Projection Method	Angles RMS error (degree)	Areas RMS error (unit length ²)	Lengths RMS error (unit length)
Harmonic / square	0.2129	0.0273	0.2312
Harmonic / circle	0.3373	0.0264	0.2014
Low-Stretch	0.3704	0.0264	0.2061
LSCM	0.1730	0.0267	0.2114
ASAP	0.1740	0.0267	0.2123
ARAP	0.1729	0.0267	0.2117

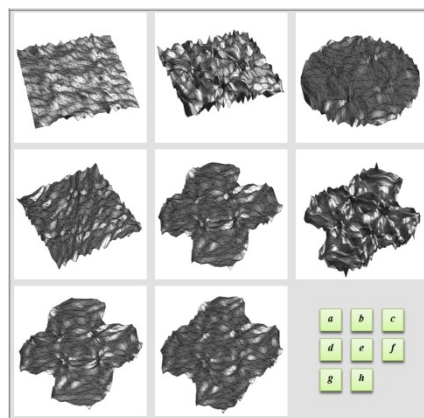


Figure 14 Surface texture imposed onto different UV-domains of the egg-box surface using; (a) Traditional projection, (b) square boundary harmonic projection, (c) circle boundary harmonic projection, (d) low-stretch projection, (e) LSCM projection, (f) ABF projection, (j) ASAP projection and (h) ARAP projection.

Table 4. Angles, areas, lengths root mean square errors between the 3D mesh and the UV mesh for the egg-box Surface

Projection Method	Angles RMS error (degree)	Areas RMS error (unit length ²)	Lengths RMS error (unit length)
Harmonic / square	0.2493	0.0392	0.3187
Harmonic / circle	0.2688	0.0380	0.2863
Low-Stretch	0.4626	0.0379	0.2855
LSCM	0.0847	0.0381	0.2880
ASAP	0.0884	0.0381	0.2880
ARAP	0.1625	0.0381	0.2876

Tables 5 and 6 shows different surface texture parameters calculated using equation 11-14 as explained in the previous section.

Table 5. Some of the global statistical parameters for the for the wavy Surface

Projection Method	<i>Sa</i>	<i>Sq</i>	<i>Ssk</i>	<i>Sku</i>
Traditional projection	0.0696	.0806	-1.3134	1.8492
Harmonic / square	0.0752	0.0868	1.3011	1.8062
Harmonic / circle	0.0761	0.0880	1.2916	1.7710
Low-Stretch	0.0754	0.0871	1.3004	1.8030
LSCM	0.0757	0.0877	1.2954	1.7817
ABF	0.0756	0.0874	1.2942	1.7795
ASAP	0.0754	0.0874	1.2970	1.7871
ARAP	0.0758	0.0876	1.2935	1.7769

Table 6. Some of the global statistical parameters for the for the egg-box Surface

Projection Method	<i>Sa</i>	<i>Sq</i>	<i>Ssk</i>	<i>Sku</i>
Traditional projection	0.0449	0.0544	1.4843	2.5234
Harmonic / square	0.0746	0.0862	1.2985	1.7967
Harmonic / circle	0.0748	0.0864	1.2966	1.7904
Low-Stretch	0.0744	0.0859	1.2994	1.8007
LSCM	0.0738	0.0857	1.3084	1.8261
ABF	0.0744	0.0860	1.2990	1.7979
ASAP	0.0740	0.0859	1.3056	1.8170
ARAP	0.0744	0.0860	1.2989	1.7981

B. Bioengineering surfaces

After the initial application of various projection algorithms to computer generated freeform surfaces, these algorithms were applied on real surface measurement data. The data were obtained from coordinate measuring machine (CMM) measurement representing a portion of hip replacement components. Two surfaces were acquired from the CMM and represented by 3D triangular meshes; the first surface has 3380 vertices and 6591 faces, and the second surface has 7182 vertices and 14108 faces (triangles). After the initial measurement of the two surfaces, an additional texture is imposed onto the surfaces to emphasise the effect of projection on surface characterisation. These two measured surfaces are shown in figure 15 we refer to these two surfaces as HipJoint-pt1 and HipJoint-pt2 as shown in figure 15(a) and (b) respectively.

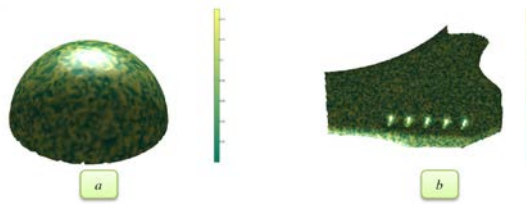


Figure 15 Bioengineering surfaces represented by 3D triangular meshes; (a) The HipJoint-pt1 surface and (b) The HipJoint-pt2 surface.

Fixed boundaries and free boundary projection algorithms were applied to calculate the 2D UV-domains for these two surfaces. Then the surface texture is projected back on these planar domains and the result of these various algorithms for both surfaces are shown in figures 16-19. The RMS errors for the main surface metric between the 3D surface and its 2D counterpart are calculated in tables 7 and 8.

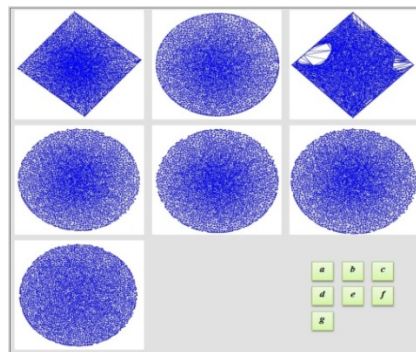


Figure 16 Projection results (UV-domains) of the HipJoint-pt1 surface using; (a) square boundary harmonic projection, (b) circle boundary harmonic projection, (c) low-stretch projection, (d) LSCM projection, (e) ABF projection, (f) ASAP projection and (g) ARAP projection.

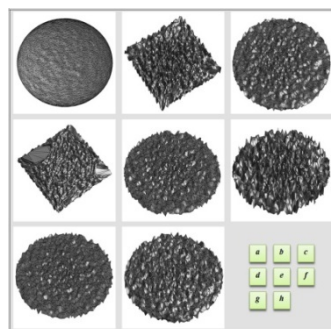


Figure 17 Surface texture imposed onto different UV-domains of the HipJoint-pt1 surface using; (a) Traditional projection, (b) square boundary harmonic projection, (c) circle boundary harmonic projection, (d) low-stretch projection, (e) LSCM projection, (f) ABF projection, (j) ASAP projection and (h) ARAP projection.

Table 7. Angles, areas, lengths root mean square errors between the 3D mesh and the UV mesh for the HipJoint-pt1 surface

Projection Method	Angles RMS error (degree)	Areas RMS error (unit length ²)	Lengths RMS error (unit length)
Harmonic / square	0.2148	0.5826	1.2085
Harmonic / circle	0.0889	0.5823	1.1914
LSCM	0.0130	0.5823	1.1914
ASAP	0.0128	0.5823	1.1917
ARAP	0.1038	0.5823	1.1957

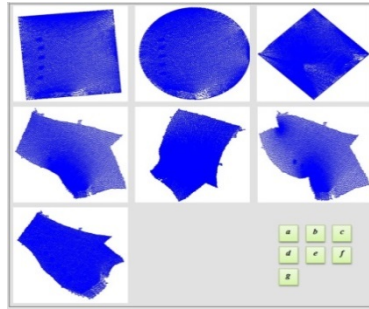


Figure 18 Projection results (UV-domains) of the HipJoint-pt2 surface using; (a) square boundary harmonic projection, (b) circle boundary harmonic projection, (c) low-stretch projection, (d) LSCM projection, (e) ABF projection, (f) ASAP projection and (g) ARAP projection.

Table 8. Angles, areas, lengths root mean square errors between the 3D mesh and the UV mesh for the HipJoint-pt2 surface

Projection Method	Angles RMS error (degree)	Areas RMS error (unit length ²)	Lengths RMS error (unit length)
Harmonic / square	0.4307	0.1475	0.5808
Harmonic / circle	0.3700	0.1473	0.5707
LSCM	0.0580	0.1474	0.5796
ASAP	0.0599	0.1474	0.5796
ARAP	0.1390	0.1474	0.5786

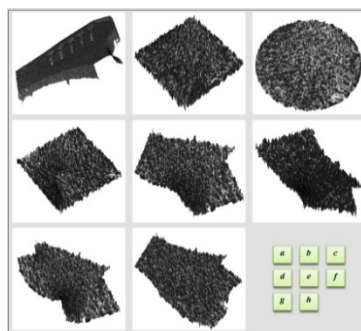


Figure 19 Surface texture imposed onto different UV-domains of the HipJoint-pt2 surface; (a) Traditional projection, (b) square boundary harmonic projection, (c) circle boundary harmonic projection, (d) low-stretch projection, (e) LSCM projection, (f) ABF projection, (j) ASAP projection and (h) ARAP projection.

Finally, different surface parameters are calculated using the equations 11-14 for the two surfaces under different projection algorithms and the results are shown in tables 9 and 10.

Table 9. Some of the global statistical parameters for the for the HipJoint-pt1 surface

Projection Method	<i>Sa</i>	<i>Sq</i>	<i>Ssk</i>	<i>Sku</i>
Traditional projection	0.0361	0.0488	1.7165	3.3650
Harmonic / square	0.0746	0.0865	1.3066	1.8227
Harmonic / circle	0.0746	0.0864	1.3063	1.8222
Low-Stretch	0.0741	0.0855	1.3025	1.8198
LSCM	0.0746	0.0865	1.3062	1.8223
ABF	0.0746	0.0865	1.3063	1.8224
ASAP	0.0747	0.0865	1.3059	1.8212
ARAP	0.0746	0.0864	1.3054	1.8198

Table 10. Some of the global statistical parameters for the for the HipJoint-pt2 surface

Projection Method	<i>Sa</i>	<i>Sq</i>	<i>Ssk</i>	<i>Sku</i>
Traditional projection	0.0328	0.0408	-1.3225	3.1000
Harmonic / square	0.0752	0.0867	1.2979	1.7964
Harmonic / circle	0.0750	0.0866	1.2990	1.7996
LSCM	0.0748	0.0864	1.3002	1.8034
ASAP	0.0750	0.0865	1.2989	1.7996
ARAP	0.0749	0.0865	1.2999	1.8028

Tables show slight changes in the texture height parameters; this is due to the fact that these parameters mainly depend on the height of the texture. In our examples, the height of the texture remains the same under different projection scheme, except for the traditional projection. However, the angles, areas and distances are significantly varied between different algorithms, which will have a significant effect on spatial parameters and other hybrid parameters. The traditional projection method produces slightly different results to the other projection methods due to the fact that the height of the texture will be distorted when projected directly onto a plane, because the traditional projection considers the texture's height in the z -direction instead of considering the height in the normal direction to the form of the surface.

All of the case studies shown in the paper, computer-simulated and real, show that texture projection methods will produce more accurate indications about the nature of the freeform surfaces and will be a more precise tool for surface characterisation.

5. Conclusions and Future Work

This research paper proposes a novel framework for freeform surfaces parameterisation. This new framework is a generalisation of the traditional model that is used to parameterise simple surfaces which are represented as height values over a regular grid. However, in this proposed model, the freeform surfaces are represented by 3D triangular meshes, and therefore could represent more range of complex surfaces. The key point of the proposed framework is to apply a projection algorithm that projects the surface from its three-dimensional world into a simpler two-dimensional world with the minimum distortions possible before calculating its parameters.

Moreover, various texture projection algorithms were investigated. These projection algorithms can be roughly divided into two main categories; the fixed-boundary (basic) algorithms and the free-boundary (advanced) algorithms. These projection algorithms attempt to project the 3D surface represented by triangular mesh into a 2D planar domain with minimum distortion in one or more in surface metrics, i.e. the distances, angles or areas.

After the surface is projected, different surface parameters can be calculated depending on the 2D planar domain. Four global statistical parameters were extended to suit surfaces represented by triangular meshes. These four parameters are the height parameters which considered being the most important parameters that can describe the surface texture. Results showed that the traditional projection method produced less accurate parameters than other projection techniques; this is because of the high distortion caused by the projection. However, all other projection methods give similar results due to the fact the parameters being calculated are influenced by the height of the residues not by the distance and angles between them. Nevertheless, spatial and features surface parameters that based on distances, angles, or the features of the surface will be affected by different projection algorithms. Such parameters are yet to be extended to accommodate new complex surfaces represented by a triangular mesh as a future work of this research. Yet another challenge to the proposed framework is to decide what is the best projection technique that has to be adopted, it still not very clear what type of projection is the best for surface characterisation, various techniques have been applied in this paper but a further investigation is needed to attempt to understand the best projection method for surface characterisation, or the best projection method for certain parameters.

The main purpose of the projection algorithm is to minimise the distortions happened when using the traditional method, i.e., subtraction of the form from the surface. However, these projection algorithms are not a distortion free and will produce some distortion in one or more of the surface metrics. Therefore, one can argue that the best way forward is to calculate the parameters directly on the surface without introducing any projection technique. This observation is completely truly, however, calculating the surface parameters directly on the surface, especially the spatial and features parameters are difficult and still not defined, and therefore, the model proposed in this paper represents an intermediate stage to calculate all the parameters.

Finally, the research shown in this paper is anticipated to have a significant impact for the characterisation of 3D printed surfaces as some of those surfaces have a freeform nature and relatively rough texture and therefore, it will be important, as a future work, to examine the projection techniques described in this paper to characterise such surfaces.

Acknowledgement:

The authors gratefully acknowledge the European Research Council under its programme ERC-2008-AdG 228117-Surfund and the UK's Engineering and Physical Sciences Research Council (EPSRC) funding of the EPSRC Centre for Innovative Manufacturing in Advanced Metrology (Grant Ref: EP/I033424/1).

References

- [1] X. Jiang *et al*, 'Paradigm Shifts in surface metrology'. Part I, Historical philosophy. Proc. R. Soc. A 463, (2007), pp: 2049–2070. doi:[10.1098/rspa.2007.1874]
- [2] X. Jiang *et al*, 'Paradigm Shifts in surface metrology'. Part II, The current shift. Proc. R. Soc. A 463, (2007), pp: 2071–2099. doi:[10.1098/rspa.2007.1873]
- [3] X. Jiang and D. J. Whitehouse, 'Technological shifts in surface metrology'. CIRP Annals - Manufacturing Technology, (2012). (<http://dx.doi.org/10.1016/j.cirp.2012.05.009>)
- [4] X. Jiang *et al*, 'Lifting wavelet algorithm for freeform surface filtering using a Gaussian prediction operator', Int. J.Precision Technology, (2013),Vol. 3, No. 3, pp.244–260.
- [5] X. Jiang *et al*, 'Multi-Scale Freeform Surface Texture Filtering using a Mesh Relaxation Scheme'. IOP, Meas. Sci. Technol. 24 (2013) 115001 (17pp)
- [6] H. S. Abdul-Rahman *et al*, 'Freeform surface filtering using the lifting wavelet transform'. Precision Engineering, Volume 37, Issue 1, January (2013), Pages 187-202.
- [7] X. Jiang *et al*, 'Freeform surface filtering using the diffusion equation'. Proc R. Soc A, Vol. 467, Issue. 2127, (2011), pp. 841–859. DOI: [10.1098/rspa.2010.0307].
- [8] J. Wang *et al*, 'Intelligent sampling for the measurement of structured surfaces', Measurement Science and Technology, (2012), 23 085006
- [9] S. Lou *et al*, 'Algorithms for Morphological Profile Filters and Their Comparison', Precision Engineering , (2012), 36(3): 414-423.
- [10] S. Lou *et al*, 'Comparison of robust filtration techniques in geometrical metrology', International Journal of Automation and Computing / Proceedings of the 18th International Conference on Automation & Computing, UK (2012), 235-240.
- [11] K. Hormann *et al*, "Mesh Parameterisation: theory and practice", SIGGRAPH Asia 2008 course notes. (2008)

- [12] A. Sheffer *et al*, “*Mesh Parameterization methods and their applications*”, Computer graphics and vision Vol. 2, No. 2 (2006), pp. 105-171.
- [13] M. Floater and K. Hormann, “Surface Parameterization: a tutorial and survey”, book chapter in “*advances in multiresolution for Geometric Modelling*”, Mathematics and Visualization (2005), pp 157-186
- [14] S. Yoshizawa *et al*, ‘A fast and simple stretch-minimizing mesh parameterization’. Proceeding of SMI '04 Proceedings of the Shape Modelling International (2004), pp. 200-208
- [15] B. Levy *et al*, ‘Least squares conformal maps for automatic texture atlas generation’. ACM SIGGRAPH conference proceedings, (2002).
- [16] L. Liu *et al*, ‘A local/Global approach to mesh parameterization’. Eurographics symposium on geometry processing (2008), volume 27, No. 5.
- [17] A. Sheffer A and E. De Sturler, ‘Parameterization of faceted surfaces for meshing using angle-based flattening’, Engineering with computers (2001), vol. 17, pp.326-337.
- [18] A. Sheffer, ‘ABF++: fast and robust angle based flattening’. ACM transactions of graphics, vol. 24, No. 2, April (2005), pp. 311-330.
- [19] M. Botsch *et al*, “*Polygon Mesh Processing*”. AK Peters Ltd (2010). ISBN: 978-1-56881-426-1
- [20] D.J. Whitehouse, “*Handbook of Surface and Nanometrology*”. Second Edition, CRC Press: Taylor and Francis Group, (2011), ISBN 978-1-4200-8201-2.
- [21] R. Leach, “*Characterisation of Areal surface texture*”. Springer (2013). ISBN: 978-3-642-36458-7.